

# Disc-Disc Encounters between Low-Mass Protoplanetary Accretion Discs

S. Pfalzner

*I. Physikalisches Institut, Universität zu Köln, Zülpicherstr. 77, 50937 Köln, Germany*

S. Umbreit, Th. Henning

*Max-Planck-Institut für Astronomie, Königstuhl 17, 69117 Heidelberg, Germany*

## ABSTRACT

Simulations of the collapse and fragmentation of turbulent molecular clouds and dense young clusters show that encounters between disc-surrounded stars are relatively common events which should significantly influence the resulting disc structure. In turn this should alter the accretion rate of disc matter onto the star and the conditions under which planet formation occurs. Although the effects of star-disc encounters have been previously investigated, very little is known about encounters where both stars are surrounded by discs. In this paper encounters of such disc-disc systems are studied quantitatively. It is found that for low-mass discs ( $M_D = 0.01 M_\odot$ ) the results from star-disc encounters can be straightforwardly generalized to disc-disc encounters as long as there is no mass transport between the discs. Differences to star-disc encounters occur naturally where significant amounts of matter are transported between the discs. In this case it is found that although the mass distribution does not change significantly, matter caught onto highly eccentric orbits is transported surprisingly far inside the disc. The captured mass partly replenishes the disc, but has a much lower angular momentum. This can lead to a reduction of the angular momentum in the entire disc and thus considerably increased accretion shortly after the encounter as well as in the long term.

*Subject headings:* accretion, accretion disks — circumstellar matter

## 1. Introduction

Numerical simulations of the fragmentation of molecular clouds produce many examples of interactions between fragments with disc-like structures (Bate et al. 2002) demonstrating

that encounters might be important in the early epochs of star formation. Even in the later stages of the star formation process, it is found that a star is likely to undergo at least one encounter closer than 1000AU during the lifetime of its disc (Scally & Clarke 2001). Recent simulations of the ONC cluster indicate that at least 20% of the stars undergo encounters closer than 300AU during the first 3Myrs of the cluster development (Olczak et al. in prep.). Naturally such encounters will influence the mass and angular momentum distribution in the disc. The total mass of - and the mass distribution within - the disc after an encounter are important, as this directly influences the likelihood of the formation of planetary systems. The change of the angular momentum distribution due to an encounter is of relevance since it is still unclear how the disc loses enough angular momentum that accretion of matter onto the star is possible. Although it is unlikely that encounters are the dominant source of angular momentum loss, their contribution is probably not negligible.

Because encounters where only one of the stars is surrounded by a disc - so called star-disc encounters - are less complex than the situation, where both stars are surrounded by discs - in the following called disc-disc encounters -, it is not surprising that past investigations have concentrated on star-disc encounters. To our knowledge only Watkins et al.(1998a,b) investigated encounters between two disc-surrounded stars. However, they focussed on the likelihood of the formation of multiple systems in the case of heavy discs and not on the discs as such.

Over the last ten years, the investigations of star-disc encounters have progressed from distant encounters (Ostriker 1994, Larwood 1997), and a qualitative approach of closer encounters (Heller 1995, Hall et al. 1996, Boffin et al. 1998, Watkins et al. 1998a,b) to a more quantitative knowledge of how the mass distribution and the angular momentum in the disc are affected by star-disc encounters (Pfalzner 2003, 2004).

However, as stars tend to form in clusters, it is at least as likely - perhaps even more likely - that in such an encounter *both* stars are surrounded by a disc. Most of the above mentioned star-disc encounter investigations can only speculate on the extent to which their results would be applicable to encounters where both stars are surrounded by a disc.

It is the aim of this paper to clarify this point quantitatively and to determine the conditions for which the results from star-disc encounters can be generalized to disc-disc encounters. In this paper, tidal effects in encounters between two stars both surrounded by low-mass discs are studied numerically in detail. A systematic study will be presented for low-mass discs, where simple N-body simulations suffice. It is demonstrated that for encounters of low-mass disc without mass exchange between the discs, there is no real difference to star-disc encounters in terms of mass and angular momentum transport. In this case, the results for star-disc encounters can be generalized to disc-disc encounters. Moreover, for the case where mass is exchanged between the discs, it is demonstrated that the additional mass alters the mass distribution only slightly. However, because the disc gains mass via the captured

material the total mass loss in the disc is less than in an equivalent star-disc encounter. On the other hand, the angular momentum is still reduced as the captured mass has a much smaller angular momentum than that of the original disc material. In section 3.3 and 3.4 the effects of viscosity, pressure and self-gravity on the mass and angular momentum loss in heavier discs are examined followed by a discussion in section 4.

## 2. Initial conditions and numerical methods

The results reported here are obtained from the disc simulations using 10 000 pseudoparticles each as tracers of the observed gas. These type of simulations are computationally expensive, so that higher resolution simulations can only be performed for special cases. Simulations using 1 million particles (see Fig.1) revealed only minor differences in the global features of interest, justifying the choice of lower particle number for the parameter studies.

### 2.1. Initial conditions

In the simulations, both stars are allowed to move freely and the masses of the stars are varied in the different encounters between  $M_* = 0.1M_\odot$  and  $1.5M_\odot$ , where in most cases one of the stars has a mass  $M_* = 1M_\odot$ . The discs extend in all simulations to 100 AU. As customary for such simulations there exists a inner gap from the star to 10% of the disc size. The gap of 10 AU prevents additional complex calculations of direct star/disc interactions and saves computer time. In addition, particles are removed from the calculation and added to the star mass if they come closer than 1AU to the stars. This overestimates accretion but avoids the simulation becoming prohibitively slow in order to model the close orbit of just one particle correctly. In the low-mass case, treated in Section 3, we chose  $M_D = 0.01M_\odot$  as this is a typical mass value of observed discs around young solar-type stars(Mannings & Sargent 1997). The density distribution in the disc is given by

$$\rho(r, z) = \rho_0(r) \exp\left(-\frac{z^2}{2H(r)^2}\right),$$

where  $H(r)$  is the local vertical half-thickness of the disc, which depends on the temperature, and  $\rho_0(r)$  is the mid-plane density with  $\rho_0(r) \sim 1/r^2$  giving a surface density of  $\Sigma \sim 1/r$ . For the  $M_D = 0.01 M_\odot$  case  $\rho_0(r) = 1.3 \cdot 10^{-10} \text{ g/cm}^3$  at  $r=1 \text{ AU}$ .

The periastra of the encounters are chosen between 100 and 350 AU. As the discs extend to  $r_D = 100 \text{ AU}$ , this covers the parameter space from penetrating to distant encounters.

As described by Heller (1995) the obtained results can be generalized for other mass distribution within the disc by applying appropriate scaling factors.

## 2.2. Numerical methods

Including pressure and viscous forces and/or self-gravity increases the computational expense. Therefore, a test particle model is used for the limited parameter studies in the first part of the paper. Here the disc particles only feel the force of the two stars, but in order to go beyond restricted 3-body simulations, the forces of the gas particles onto the stars are included too. This means that particles close to the center of the disc can influence the movement of the star. Due to their low mass, the influence of single particles will generally small. However, if the mass distribution near the center becomes in any way asymmetric (for example by captured material) this can influence the movement of the star. As Pfalzner(2003) showed the movement of the central star plays a vital role in the formation of the second spiral arm in the disc. Thus there is always a feedback between disc and star.

One could question this approach of excluding pressure and viscous forces and/or self-gravity, especially in disc-disc encounters. However, the comparison with our simulations that include all above mentioned effects (see Section 4) show that this simplification is justified as long as one is only studying such global features as mass transport and restricts oneself to low-mass discs. For higher mass discs ( $M_D \gg 0.01M_*$ ) the simple test particle model no longer suffices. In section 4 the effects of pressure and viscous forces as well as self-gravity are considered. Selected smoothed particle hydrodynamics (SPH) simulations are performed to give an qualitative assessment of these effects for high-mass discs in general. Details of the numerical method for both kind of simulations are described in Pfalzner(2003).

## 3. Disc-disc interaction

A typical example of an encounter where both stars are surrounded by discs is shown in Fig.1. In this example both stars are of equal mass,  $M_1^* = M_2^* = 1M_\odot$ , as are the discs,  $M_D^1 = M_D^2 = 0.01M_\odot$ . The stars move on a parabolic orbit, the encounter is prograde, coplanar, with both discs rotating in the same direction and the distance between the stars at the periastron is 150 AU. After approximately  $t=700$  yrs a tidal bridge develops, which is equivalent to the appearance of the first spiral arm in star-disc encounters. The picture at  $t=800$  yrs shows the appearance of two counter tidal tails. At  $t=1300$  yrs it can be seen

how the disc develops independently towards its new equilibrium states. The resulting discs illustrate the characteristic tightly wound spiral arm pattern very similar to that seen in the outer discs recently observed by Grady et al. (2001), Clampin et al.(2003) and Fukagawa et al. (2004).

We varied the relative periastron distance,  $r_{peri}/r_{disc}$ , and eccentricity of the orbit in our simulations of such encounters. The mass and angular momentum distribution as well as the total mass and angular momentum loss in the disc after the encounter were analyzed and the results of disc-disc compared with those of star-disc encounters.

### 3.1. Mass distribution

It is important to know the total disc mass as well as the mass distribution within the disc after the encounter in the context of planet formation. If these quantities are considerably changed by encounters, this could have serious implications for the possible development of planetary systems. For example, in the extreme case of a very close encounter the stars might be completely stripped of their discs or the disc could become truncated at a certain radius, thus prohibiting planet formation either altogether or beyond a certain radius. In the more likely case of a distant encounter, it is known from star-disc encounter simulations that the central region of the disc remains relatively unaffected, but the perturbation of the outer disc could lead to planets on highly eccentric orbits. The recently discovered planetoid 2003 VB12 (Trujillo et al. 2004) on an eccentric orbit with a perihelion distance of 70AU might possibly have formed through such an interaction (Keynon & Bromley 2004).

Fig.2 shows a closeup of the snapshot at  $t= 1300$  yrs of an encounter similar to Fig.1 but with a periastron distance of 150 AU and with the smaller spatial resolution of 10 000 particles per disc; which illustrates the mass originating from disc 1 (grey) and the mass that star 1 captured from disc 2(black). As the captured mass is clearly visible throughout the entire disc, this seems to imply a quite altered mass distribution. In Fig.3a the initial mass distribution and the distribution 1200 yrs after the encounter are shown as a function of the radial distance from the star for the example shown in Fig.2. The comparison of these two distributions gives quite a different impression than Fig.2. As in star-disc encounters, mass is lost from the outside of the disc and also transported inwards (for a detailed explanation of the dynamics see (Pfalzner 2003). Fig. 3b shows that the amount of mass caught from the other disc is nevertheless relatively small compared to the total disc mass, showing that the resulting mass distribution does not differ significantly from that in star-disc encounters. Fig.3c shows that the gain in surface density through this mass from the passing star-disc system is nearly constant at all disc radii, even showing a small rise towards the

center. Since the above situation might not be a typical example, we compared the change in the mass distribution in star-disc with that in disc-disc encounters for several different encounter situations varying the periastron and the star masses. The result is that the mass distributions after the encounter are (also quantitatively) like those in star-disc encounters in all investigated cases. This is found both for prograde as well as retrograde encounters. In cases where there is a change in the density profile and/or a truncation of the disc in star-disc encounter, this will equally apply to disc-disc encounters. Results concerning the mass distribution from star-disc encounters can therefore be generalized for disc-disc encounters. Investigations of the mass distribution in star-disc encounters can for example be found in Pfalzner(2003); the disc size in such a situation has been analyzed in Pfalzner et al.(subm).

However, not all is the same for star-disc and disc-disc encounters. Fig.3c compares the mass losses from the disc with the mass gained from the other disc as a function of the radial distance from the star. It can be seen that in this example the captured mass is only about a factor 3 smaller than the mass transported within the disc itself. More importantly, the captured material is partly transported very far inside the disc. This can have two consequences i) the possibility of mixing material of different chemical composition and ii) influencing the movement of the central star and therefore the further development of the entire disc. Both effects would need further investigation.

This raises the obvious question: Under which conditions is mass transported between both discs? To answer this question we performed a number of encounter simulation with different encounter parameters.

In Fig.4 the mass of the disc around star 2 captured by star 1 is shown in encounters for different periastron distances, where both stars are of equal mass,  $M_1^* = M_2^* = 1M_\odot$ . It can be seen that for hyperbolic encounters, a much smaller mass transfer occurs between the disc than for parabolic encounters - which can be up to 20 %. This is caused by the fact that the interaction time in a hyperbolic encounter is much shorter than in a parabolic one, leaving less time for the star to actually bind matter. This raises the question, whether in a parabolic encounter the loss of disc material can be compensated by the gain of mass from the other disc.

To answer this we compare the mass loss from disc 1 to the gain in matter captured from disc 2. In Fig. 4b it can be seen that in the parameter range of  $r_{peri}/r_{disc} = 1 - 2.25$  the mass loss is at least two-times larger than the gain through captured mass: in other words the gain in disc mass cannot completely replenish the disc. It can also be seen that the difference becomes larger for closer encounters.

In a second step we followed this point up by measuring the mass loss and angular momentum loss in star-disc and disc-disc encounters for 9 different periastron distances. Fig.5 compares the total mass loss in star-disc encounters to that in disc-disc encounters. Not surprisingly due to the mass gained from disc 2, the mass loss in disc-disc encounters is generally less than that in star-disc encounters.

It is curious that the mass exchange between the disc significantly alters the total mass loss, but does not seem to affect the mass distribution so much. The reason for this is the way the captured mass is distributed. Fig.6 shows the surface density of the captured mass for different encounter periastra. Obviously the captured mass is concentrated closer to the star for smaller encounter parameters. This means when more mass is captured, most of it is hidden in the steep density gradient near the central star, whereas only a small amount of the captured matter resides in the outer regions of the disc.

### 3.2. Angular momentum

The angular momentum and the angular momentum per particle are important in the context of accretion: the smaller the angular momentum the easier the matter can be accreted.

It turns out that for the angular momentum loss in a disc-disc scenario the trends are considerably different from that of the mass loss. Although the angular momentum loss is reduced in comparison to the situation in star-disc encounters (see Fig.5b), it is so to a much lesser degree than the mass loss. The reason is that after some complex path in the capturing process (see Fig.7a), the captured particles settle on the above mentioned highly eccentric orbits (see Fig.7b) around the star 1 with the same direction of rotation they had before around the star 2. Most ( $\sim 80\%$ ) of the captured particles have eccentricities above 0.8 and almost none of them have orbits less eccentric than 0.4.

Consequently the captured particles have a *low angular momentum* relative to the star, so that the total angular momentum loss of the disc does not differ much from that in star-disc encounters. This becomes even more apparent if one looks at the specific angular momentum. In Fig. 8a the specific angular momentum per mass unit is shown for the encounter of Fig.2. It can be seen that in this particular case, the angular momentum of the captured matter is only about half that of the other particles throughout the disc apart from the innermost 15 AU. What is particularly striking is that for such close encounters the angular momentum of the particles originally belonging to the disc is reduced from the disc edge down to about 40AU, whereas the angular momentum reduction of the captured material

reaches into the disc to about 10-12AU. So for very close encounters the determination of the angular momentum of the captured material is critical due to the inner cut-off of the disc at 10AU. For these cases ( $r_{peri}/r_{disc} < 1.1$ ) simulations with better resolution of the inner disc area would be necessary.

Fig. 8b shows the angular momentum per unit mass of the captured material in encounters with different periastra. In the outer regions the angular momentum is always much smaller than in the unperturbed disc more or less independent of the encounter periastron. Here the angular momentum is always about half that of the unperturbed disc. In the inner regions of the disc the reduction seems to become slightly more for closer encounters. The simulations probably under-resolve this effect here, since particles that approach the star closer than 1AU are removed from the calculation in order to save computer time. These particles might either be accreted or go on highly eccentric orbits too.

### 3.3. Pressure, viscosity and self-gravity effects

A common objection to the above approach is the neglect of pressure, viscosity and self-gravity in the disc. To justify this simplification we performed additional simulations including pressure and viscosity effects, and then self-gravity.

The initial temperature profile was chosen using the thin-disk approximation with a scale height of the disk of  $H(r) = r/H_0 = r/33$ , where  $H_0$  is a dimensionless constant, and an isothermal equation of state giving  $T(r) \sim 1/r$ . Using the fact that  $r/H = v_\phi/c_s$ , with  $c_s$  being the isothermal sound speed and  $v_\phi$  the velocity component of the disk material in  $\phi$  direction,  $H_0$  simply represents the local Mach number of the disk material. Viscosity was included in the SPH scheme using the tensor description by Flebbe et al.(1994). For simplicity a constant kinematic viscosity  $\nu = 4.6 \cdot 10^6 \text{ cm}^2/\text{s}$  was used, which is related to the parameter  $\alpha$  in the standard  $\alpha$ -model by  $\nu = \alpha c_s(r) H$  with  $c_s$  being the isothermal sound speed. Since  $c_s$  is decreasing as  $1/\sqrt{r}$ , the same radial dependence holds for  $\alpha$  with a value from  $\alpha=0.16$  at 5AU to 0.036 at 100AU. The SPH-code itself is described in detail in Pfalzner (2003).

To compare the simulation without and with pressure and viscous effects is not straightforward. The problem is that there are three different competing effects occurring: altered initial distribution, pressure and viscous effects and star-disc vs. disc-disc encounter, which can influence the final outcome. The first point arises from the necessity of starting the simulation with a disc that is as close as possible to an equilibrium state including pressure and viscous forces. This disc usually deviates from the Keplerian disc with a  $1/r$ -surface density

distribution: the higher the temperature the more so. Consequently, the initial mass and velocity distribution in the encounter scenario is in this situation always slightly different to the Keplerian disc. Although the strongest effects of pressure and viscous forces are felt at the center of the disc, the disc edge is also effected: essentially the outer edge of the disc is more smeared-out and surface density near the inner edge is reduced.

It is difficult to distinguish between effects that are due to the altered initial distribution with pressure and viscous effects to those that result from both stars being surrounded by a disc. Therefore we will only compare star-disc and disc-disc encounters which start with the same initial disc including pressure and viscous forces in the calculation.

Encounter simulations were performed with three different periastra showing that despite the different initial conditions, the mass distribution after the disc-disc encounter differs very little from that of star-disc encounters. In Fig.9 the mass and angular momentum loss of these gaseous, low-mass discs is shown as function of the encounter periastron for both star-disc and disc-disc encounters. For comparison the curves fitted to the results of the simulations *without* pressure and viscous forces (Fig.5) are shown, too. It can be seen that for encounters with  $r_{peri}/r_{disc} \simeq 150$  AU, there is little difference between the mass and angular momentum loss with and without pressure and viscous forces for both the star disc and the disc-disc cases.

For  $r_{peri}/r_{disc} = 200$  AU the mass and angular momentum loss are both considerably higher in the gaseous case. In such distant encounters it is mainly the outer regions of the disc which is affected. Since the mass distribution of the initial disc is more smeared out at the edges, there is some matter outside 100 AU. This matter is easily detached from the star even in an 200 AU encounter. The reason for the higher mass and angular momentum loss in an 200AU encounter for gaseous discs is just the changed mass and velocity distribution in the initial discs.

Although the periastron dependence of the mass and angular momentum loss seems to be different for the case of gaseous discs, the relative difference between star-disc and disc-disc encounters is to be the same as in the non-gaseous case. We conclude that viscous and pressure forces seem to play a minor role in this context, which is not surprising given that pressure and viscosity effects predominantly alter the dynamics close to the stars.

Interestingly, pressure forces do not hinder the captured matter from being transported far inside the disc. There might be two reasons for this: a) the pressure is not high enough to hinder the captured material from coming far inside or b) the treatment of viscosity in SPH is not sufficient. The latter can only be tested by performing similar simulations with a grid-based hydro-code.

Fig. 10a shows that the captured mass is distributed in a similar fashion to the case without pressure and viscous forces. The main difference is that there is no maximum at around 70 AU. This might be due to the changed initial mass distribution at the outer edge. One would expect a larger difference in the inner disc where viscous and pressure effects are strongest. However, there seems to be no indication of that, apart from the fact that there are slightly fewer particles within 1 AU around the star and slightly more in the adjacent areas. The angular momentum distribution also seems little effected, but this may change on longer time scales than the present snapshot 2000 yrs after the encounter. To obtain better information about the long term fate of the matter captured close to the star, simulations including the inner 10AU area would be required.

The self-gravity of disc particles is simulated by evaluating the mutual interactions of all disc particles using a hierarchical tree code developed by Pfalzner(2003). Performing a simulation of the same encounter as before, but including the self-gravity within the disc, our simulations show that self-gravity neither influences the mass nor angular momentum transport for low mass discs. The results for the disc with  $M_D = 0.01M_\odot$  including the self-gravity within the disc are virtually identical to those of the previous section as indicated in Fig.9.

Recently, indications for high-mass discs around more massive stars have been found (Shepherd et al. 2001, Chini et al. 2004, Schreyer et al. 2002), so it is naturally of interest to see what changes to our previous arguments can be expected for higher masses. As an example, we choose a disc of mass  $M_D/M_* = 0.1$ . Again, an equilibrium solution for the disc has to be found first before allowing the two systems to interact. The most relevant effects are the smeared out edge and a slight increase in velocity in the outer parts of the disc (for a comparison of the initial conditions see Pfalzner 2003).

Simulations of such an encounter show that star 2 seems to influence the disc of star 1 at a somewhat earlier time. The reason for this lies simply in the different initial condition - there is no strict cut-off at 100 AU as before, but the edge is smeared out and particles further out are affected sooner. In addition, the increased disc mass influences the stellar orbits and the higher amount of captured matter contributes to this effect as well.

Interestingly, the time over which mass and angular momentum exchange occur after the encounter seems to be longer than for the low-mass case. This prolonged exchange time seems to be directly connected to the larger disc mass - the exchange of energy and angular momentum results in a longer period until an equilibrium is reached.

We find the same behaviour for the angular momentum and mass transfer as in above described simulations apart from a much more pronounced “eigen-evolution” of the material

remaining bound to the star, which is typical for self-gravitating discs.

#### 4. Discussion and Conclusions

In this paper the consequences of encounters between two disc-surrounded stars have been investigated. The simulations results have been compared to the well-investigated scenario where only one of the stars is surrounded by a disc. The majority of the results were obtained by performing simulations without including pressure, viscous or self-gravity effects, but additional simulations discussed in section 3.3, which do include these effects indicate that the main findings still hold when these effects are included.

The emphasis of this investigation was on the mass and angular momentum transport in such disc-disc encounters. It was found that for low-mass discs, the findings of star-disc encounters can be generalized as long as there is no significant mass exchange between the disc. It has been shown for coplanar encounters with  $r_{peri} > 100$  AU that mass exchange between discs can only be expected for nearly parabolic, close prograde encounters. For hyperbolic encounters with a periastron larger than 3 times the disc size, mass transport between the discs will be negligible. This means for the majority of hyperbolic encounters the results for the mass and angular momentum transport of star-disc encounters can be applied to disc-disc encounters.

In cases where matter is transported (mainly parabolic encounters), the additional mass alters the mass distribution only slightly. This has several reasons: For distant encounters the mass exchange is at most a few percent. This is spread more or less evenly over the whole disc area, thus having little effect on the overall mass distribution. For close encounters we find that up to 20 per cent of disc mass is captured. However, a considerable amount of this ends up very close to the star thus “hiding” in the steep density gradient near the star. On the other hand, because the disc gains mass via the captured material, the total mass loss in the disc is actually less than in an equivalent star-disc encounter.

The change in angular momentum is more subtle, since affected differently as the captured mass moves on highly eccentric orbits, getting transported far inside the disc and so has a much smaller angular momentum than the original disc material. Unlike the matter in the initial disc the angular momentum of the captured matter does not increase on average with larger distance from the star, but is nearly constant at all radii.

What consequences do these results have for the late stages of star formation and planet formation?

In the context of star formation the accretion rate onto the star is of vital importance. Since the angular momentum of the captured matter in disc-disc encounters is so much lower than that of the initial disc, accretion could be enhanced in two ways: First, as a considerable amount of the captured matter goes on orbits of high eccentricity very close to the star, this can lead to an increase of accretion shortly after the encounter. Second, long term viscous processes could lead to an exchange of angular momentum between the captured and original particles in the disc. The circularization of the orbits of the captured matter could in this way cause a reduction of the angular momentum of all the particles in the disc. This lower angular momentum could eventually facilitate the accretion process.

Of course, it would be difficult to actually observe the increased accretion, since even a parabolic encounter lasts no longer than a few hundred years. What might be observable, however, is chemical mixing, assuming the two discs are of different chemical composition.

Here only hyperbolic and parabolic encounters were investigated, but the results give some indications for cases where bound binaries are formed by the star-disc or disc-disc encounter, too: The case where both stars are surrounded by a disc would lead to a much larger decrease in angular momentum and this should lead to much higher accretion rates. So if binaries are formed in such encounters, then they will do so preferably in disc-disc encounters instead of star-disc encounters.

The notion that the development of spiral arms in gravitationally unstable discs might be an important ingredient in the formation of planets is an interesting possibility (Boss). Such instabilities facilitate the formation of planets due to both the increased density and through a velocity dispersion that facilitates dust and planetesimal growth (Rice et al. 2004). The problem with this hypothesis is that the timescales for low-mass discs to become gravitationally unstable are relatively long. By contrast, encounters seem to be much more common in dense young clusters than previously thought and lead to very similar but much stronger spiral arms on very short time scales, and are therefore a much more plausible catalyst for planet formation than instabilities alone. An additional advantage is that in disc encounters spiral arms - and possibly as well the necessary conditions for the formation of planets - occur even in low-mass discs.

As was shown in this paper the captured matter can not be expected to increase the density in the spiral arms significantly. However, because it moves on highly eccentric orbits far inside the disc, the velocity dispersion in the disc should be considerably increased. So if one accepts that spiral arms are an important ingredient for planet formation, then the two-disc interaction will be even more efficient than a star-disc encounter in creating the necessary conditions.

## REFERENCES

Bate, M. R., Bonnell, I. A., & Bromm, V. 2002, MNRAS, 336, 705

Boffin, H. M. J., Watkins, S. J., Bhattal, A. S., Francis, N., & Whitworth, A. P. 1998, MNRAS, 300, 1189

Chini, R., Hoffmeister, V., Kimeswenger, S., Nielbock, M., Nürnberg, D., Schmidtbreick, L., & Sterzik, M. 2004, Nature, 429, 155

Clampin, M., Krist, J. E., Ardila, D. R., Golimowski, D. A., Hartig, G. F., Ford, H. C., Illingworth, G. D., Bartko, F., Benítez, N., Blakeslee, J. P., Bouwens, R. J., Broadhurst, T. J., Brown, R. A., Burrows, C. J., Cheng, E. S., Cross, N. J. G., Feldman, P. D., Franx, M., Gronwall, C., Infante, L., Kimble, R. A., Lesser, M. P., Martel, A. R., Menanteau, F., Meurer, G. R., Miley, G. K., Postman, M., Rosati, P., Sirianni, M., Sparks, W. B., Tran, H. D., Tsvetanov, Z. I., White, R. L., & Zheng, W. 2003, AJ, 126, 385

Flebbe, O., Muenzel, S., Herold, H., & Ruder, H. 1994, ApJ, 431, 754

Fukagawa, M., Hayashi, M., Tamura, M., Itoh, Y., Hayashi, S. S., Oasa, Y., Takeuchi, T., Morino, J., Murakawa, K., Oya, S., Yamashita, T., Suto, H., Mayama, S., Naoi, T., Ishii, M., Pyo, T., Nishikawa, T., Takato, N., Usuda, T., Ando, H., Iye, M., Miyama, S. M., & Kaifu, N. 2004, ApJ, 605, L53

Grady, C. A., Polomski, E. F., Henning, T., Stecklum, B., Woodgate, B. E., Telesco, C. M., Piña, R. K., Gull, T. R., Boggess, A., Bowers, C. W., Bruhweiler, F. C., Clampin, M., Danks, A. C., Green, R. F., Heap, S. R., Hutchings, J. B., Jenkins, E. B., Joseph, C., Kaiser, M. E., Kimble, R. A., Kraemer, S., Lindler, D., Linsky, J. L., Maran, S. P., Moos, H. W., Plait, P., Roesler, F., Timothy, J. G., & Weistrop, D. 2001, AJ, 122, 3396

Hall, S. M., Clarke, C. J., & Pringle, J. E. 1996, MNRAS, 278, 303

Heller, C. H. 1995, ApJ, 455, 252

Keynon, S. J. & Bromley, B. C. 2004, Nature, 432, 598

Larwood, J. D. 1997, MNRAS, 290, 490

Mannings, V., Sargent, A.I., 1997, ApJ, 490, 792

Olczak, C., Pfalzner, S., Eckart, A., in preparation

Ostriker, E. C. 1994, *ApJ*, 424, 292

Pfalzner, S. 2003, *ApJ*, 592, 986

—. 2004, *ApJ*, 602, 356

Pfalzner, S., Vogel, P., Scharwächter, J., Olczak, Ch., to be published in *A&A*.

Rice, W. K. M. and Lodato, G. and Pringle, J. E. and Armitage, P. J. and Bonnell, I. A., 2004, *MNRAS*, 355, 543

Scally, A. & Clarke, C. 2001, *MNRAS*, 325, 449

Schreyer, K., Henning, T., van der Tak, F. F. S., Boonman, A. M. S., & van Dishoeck, E. F. 2002, *A&A*, 394, 561

Shepherd, D. S., Claussen, M. J., & Kurtz, S. E. 2001, *Science*, 292, 1513

Trujillo, C. A. and Brown, M. E. and Rabinowitz, D. L. and Geballe, T. R., 2004  
AAS/Division for Planetary Sciences 36

Watkins, S. J., Bhattacharjee, A. S., Boffin, H. M. J., Francis, N., & Whitworth, A. P. 1998,  
*MNRAS*, 300, 1205

—. 1998, *MNRAS*, 300, 1214

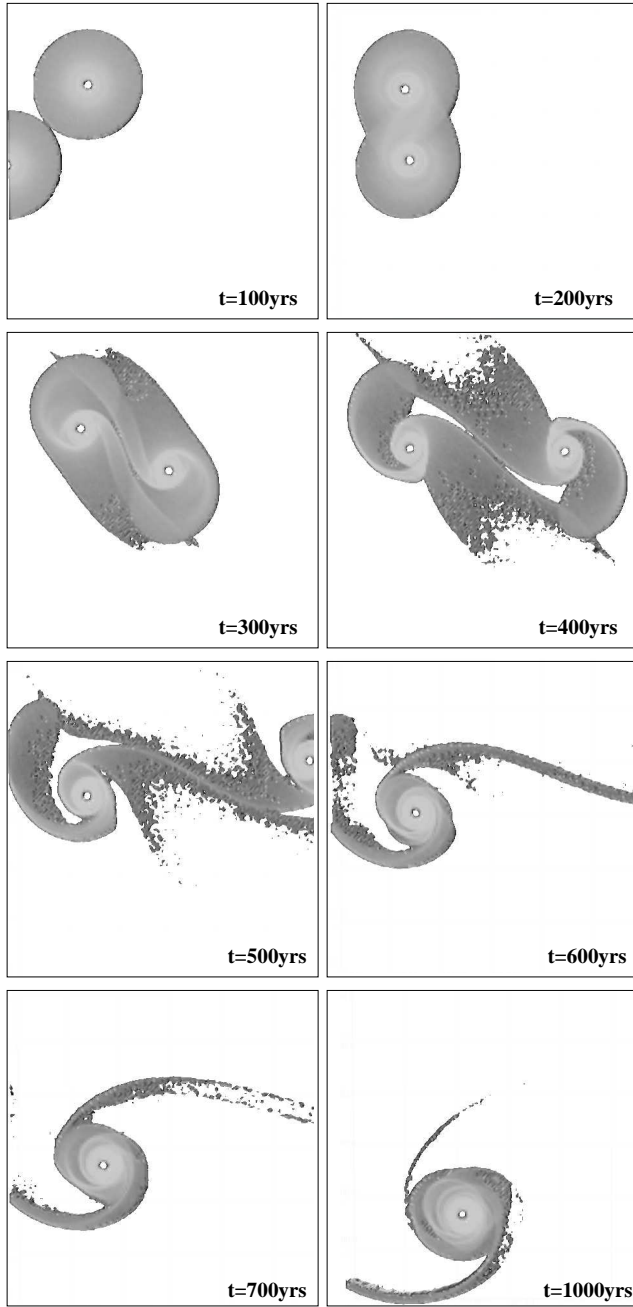


Fig. 1.— Typical example of the simulation of an encounter between two low-mass discs. The simulation has been performed with 500 000 particles per disc. Shown are density plots where the dark areas represent low density regions.

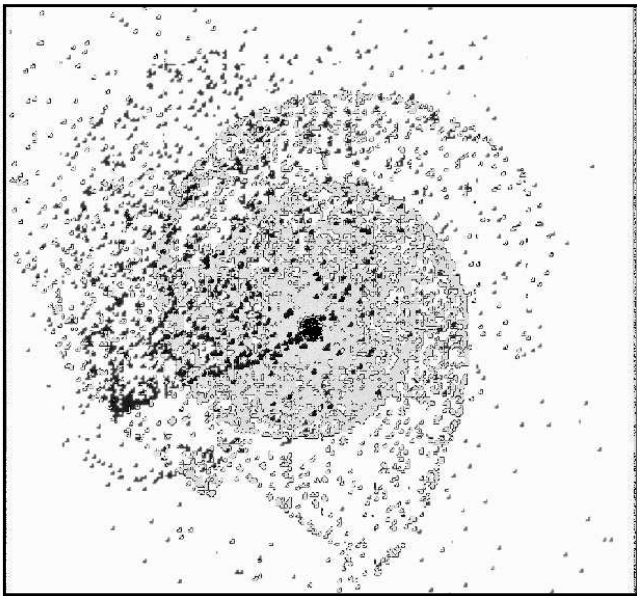


Fig. 2.— Closeup of one of the discs at  $t = 1300$  yrs after an parabolic encounter with  $M_1 = M_2 = 1M_\odot$  and  $r_{peri}/r_{disc}=1.5$ . The particles in grey are from the original disc of the considered star, whereas the particles in black originate from the disc of the other star.

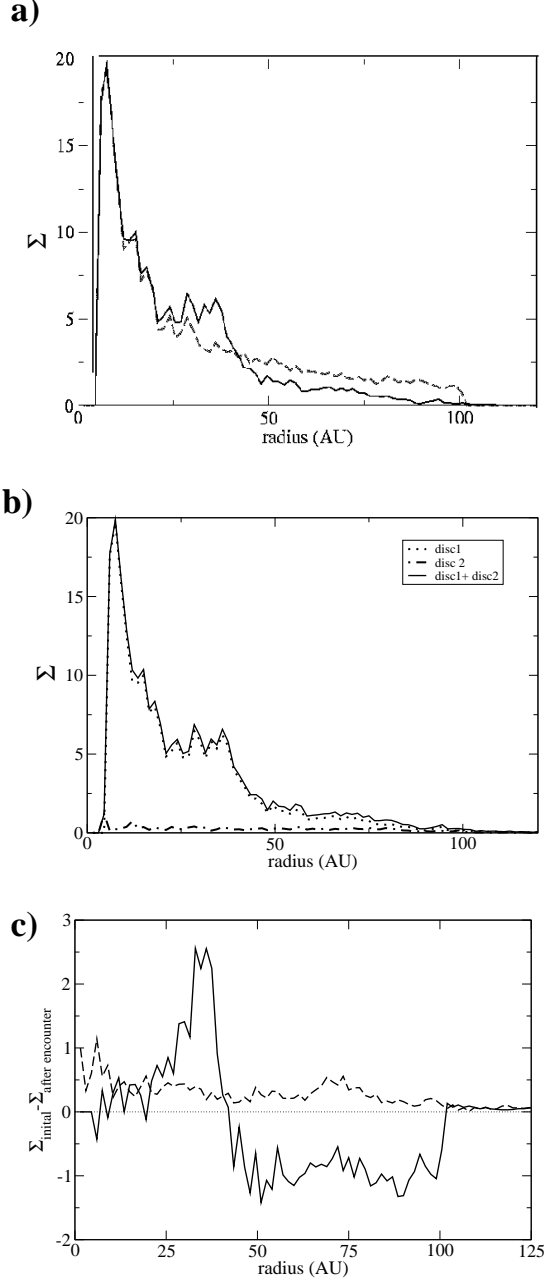


Fig. 3.— Change of the surface density  $\Sigma$  in the disc as a function of the radial distance. The surface density is given in units of  $10^{-6} M_{\odot}/\text{AU}^2$  corresponding to  $8.9 \text{ g/cm}^2$ . In a) the original surface density is shown as dashed line, whereas the surface density distribution after the encounter is shown as solid line. b) shows how the total surface density (solid line) after the encounter contains matter originally belonging to disc 1 (dotted line) and matter originating from disc 2 (dash-dotted line). It demonstrates that the contribution from the disc 2 is relatively small. However, in the change of the distribution ( $\Sigma_{\text{initial}} - \Sigma_{\text{after encounter}}$ ) the particles from disc 2 (dashed line) play a non-negligible role compared to those from disc 1 (solid line) as c) shows.

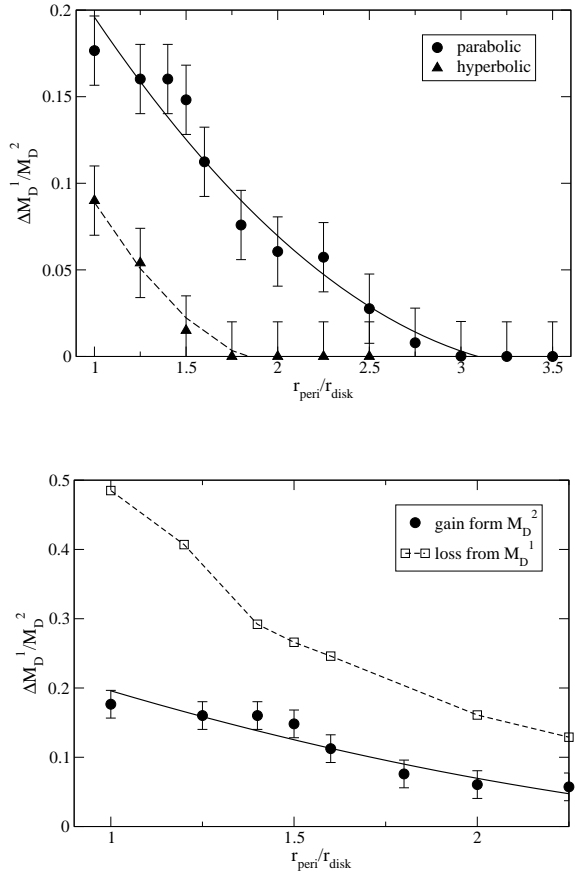


Fig. 4.— Mass transferred from the disc around star 2 to the disc around star 1 in an encounter  $M_1 = M_2 = 1M_\odot$  as a function of  $r_{peri}/r_{disk}$ . In a) the mass transfer in parabolic encounters is compared to that in hyperbolic encounters. b) shows a comparison of the loss of matter originally belonging to disc 1 with the gain of matter through capture of matter originally belonging to disc 2.

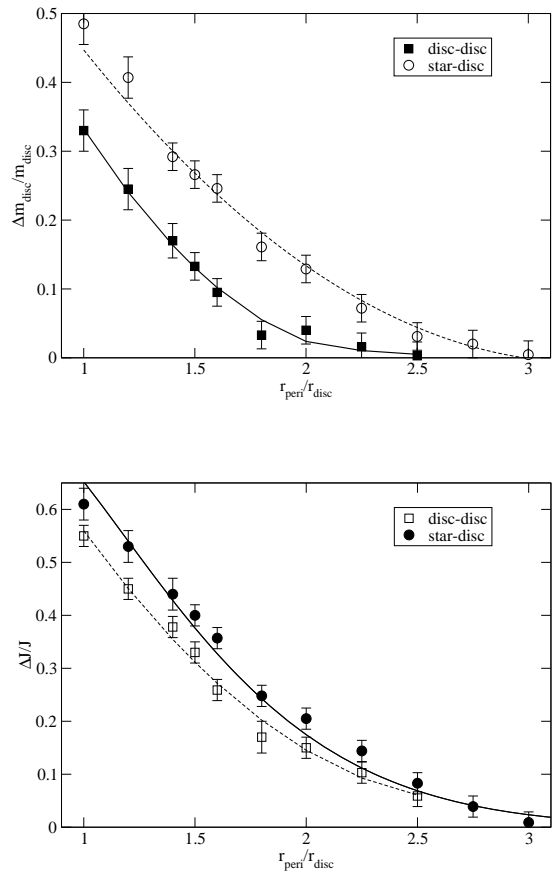


Fig. 5.— Dependence of the a) mass and b) angular momentum loss in the disc as a function of  $r_{peri}/r_{disc}$  for an encounter of two stars of  $M_1 = M_2 = 1M_\odot$

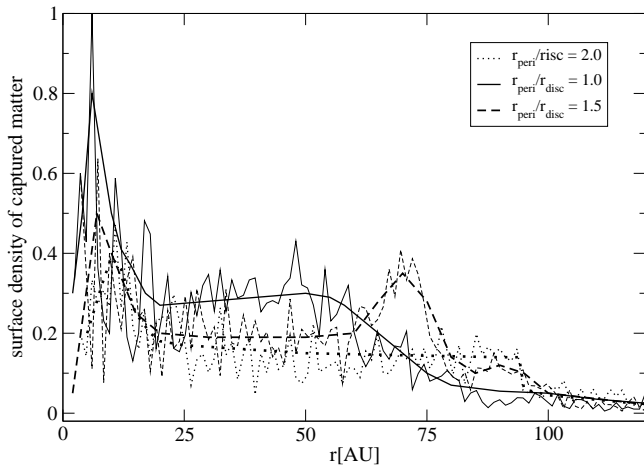


Fig. 6.— Surface density of the captured mass as function of the radial distance from star 1 after encounters with  $M_*^1 = M_*^2 = 1M_\odot$  and a periastrion distance of 100AU, 150AU and 200AU.

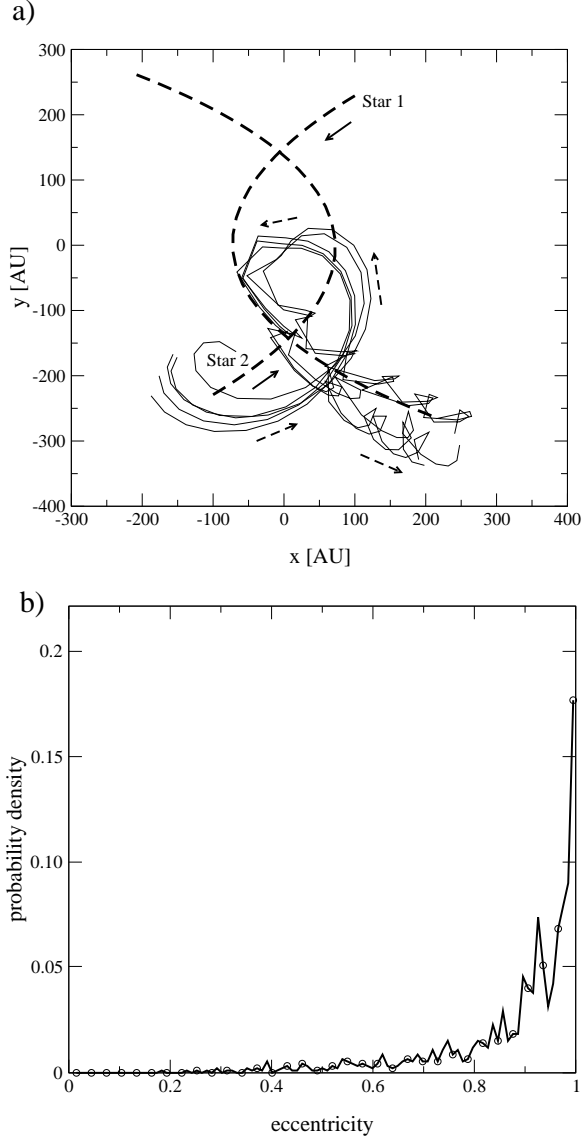


Fig. 7.— a) shows the trajectories of some particles being captured by the central star (star 1) relative to the center of mass of the stars (solid lines). The dashed lines represent the orbits of the stars. The captured particles go on quite complex trajectories and end up in highly eccentric orbits around star 2 with the same direction of rotation they had before around the other star. b) illustrates the eccentricity distribution of the captured particles. Most of them end up in highly eccentric orbits with eccentricities higher than 0.8. Almost none of them has eccentricities below 0.4.

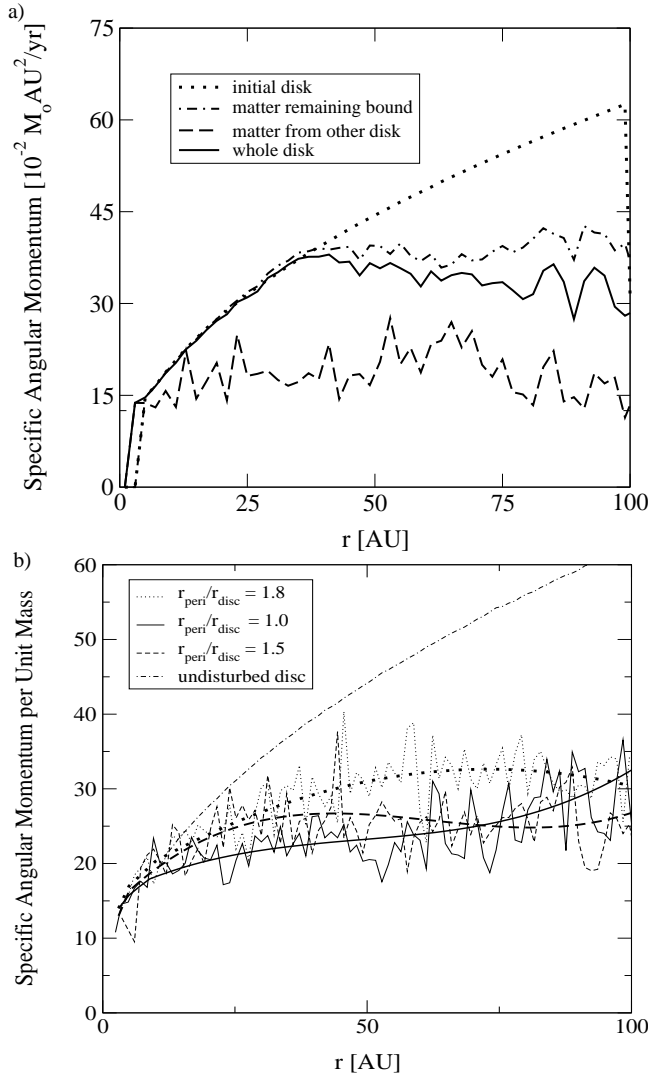


Fig. 8.— Change of specific angular momentum per particle during disc-disc encounters. a) Shows the initial angular momentum per particle before the encounter(dotted line), the particles remaining bound to the primary (dotted-dashed line), the particles that come from the passing star(dashed line) and all particles together(solid line) as a function of the radial distance from star 1 for the case in Fig.1. b) illustrates the specific angular momentum per particle of the captured mass for different encounter periastra.

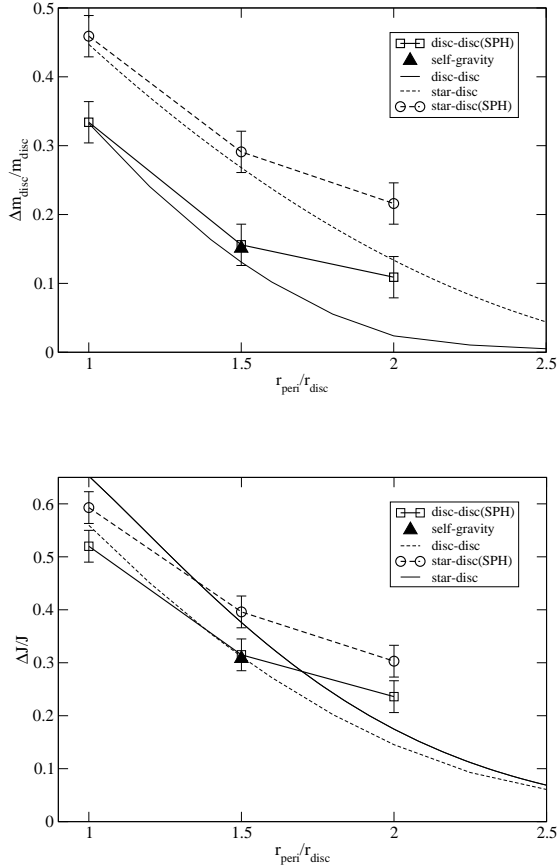


Fig. 9.— Comparison between disc-disc(squares, drawn lines) and star-disc(circles, dashed lines) encounters simulations with pressure and viscous forces included. a) shows the mass loss and b) the angular momentum loss as a function of the periastron. In both figures the fit to the results from the encounters without pressure and viscous forces of Fig.5 where marked by drawn and dashed lines without symbols for comparison. The triangle indicates the result of a simulation where the self-gravity of the disc is included.

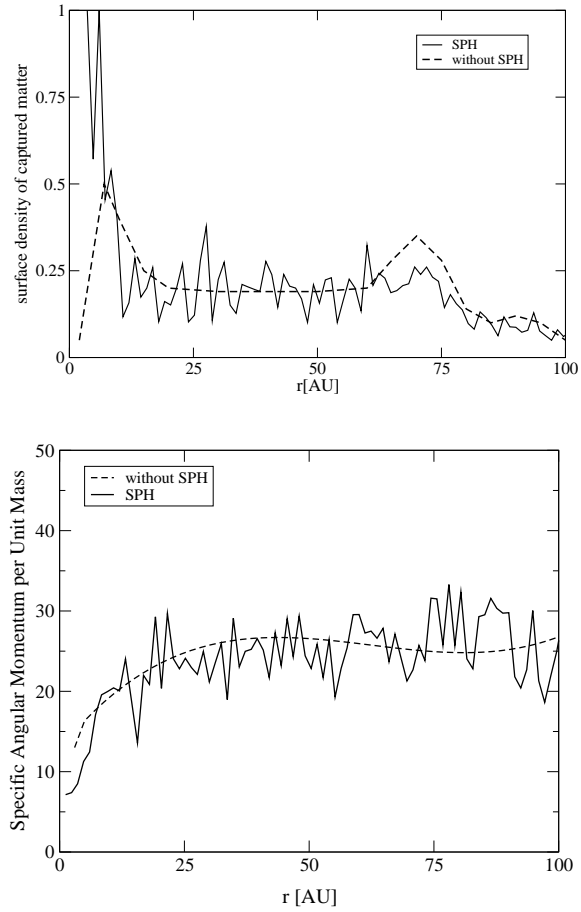


Fig. 10.— Comparison of encounter simulations with (SPH) and without pressure and viscous forces. In the encounter both stars were surrounded by a disc and the encounter was parabolic with a periastron of 150AU. a) shows the surface mass distribution of the captured material in both cases. b) shows the distribution of the specific angular momentum in both cases.